METRICA
METRology Institutional CAtalog

ISTITUTO NAZIONALE DI RICERCA METROLOGICA
Repository Istituzionale

Experimental determination of the dynamic elastic modulus of polymeric soft materials in an extended frequency range: A supported free loading-mass method

This is the author's accepted version of the contribution published as:

Original
Experimental determination of the dynamic elastic modulus of polymeric soft materials in an extended frequency range: A supported free loading-mass method / Prato, A., Romeo, R., Cuccaro, R., Schiavi, A.. - In: MEASUREMENT. - ISSN 0263-2241. - 199:(2022), p. 111587. [10.1016/j.measurement.2022.111587]

Availability:
This version is available at: 11696/74900 since: 2022-11-15T09:27:52Z

Publisher:
ELSEVIER SCI LTD

Published
DOI:10.1016/j.measurement.2022.111587

Terms of use:

This article is made available under terms and conditions as specified in the corresponding bibliographic description in the repository

Publisher copyright

(Article begins on next page)

16 November 2026

Experimental determination of the dynamic elastic modulus of polymeric soft materials in an extended frequency range: A supported free loading-mass method

Prato Andrea, Romeo Raffaella, Cuccaro Rugiada, Schiavi Alessandro

Published on: Measurement, Volume 199, August 2022, 111587

Abstract

In this paper, an experimental test method to accurately measure the complex dynamic elastic modulus of soft materials designed for anti-vibration purposes over a wide frequency range with high resolution at low uncertainty levels is proposed and applied to six polymeric soft materials. The proposed experimental technique, based on primary laser-Doppler velocimetry, is conceived to provide the uniaxial dynamic modulus of these materials on the basis of the exact solution of the Newton's second law differential equation of a free loading-mass supported by a spring-damper system and subjected to an underlying dynamic stress. After a preliminary characterization with different standard procedures, the dynamic elastic modulus and damping properties of the six materials are investigated over a frequency range of 25-1000 Hz. The overall expanded uncertainty, on average around 3 %, is determined from five repeated measurements including the instrumental uncertainty. Results are compared with the standard ones.

Keywords: dynamic complex elastic modulus, laser-Doppler velocimetry, polymeric soft materials.

1. Introduction

Polymeric soft materials are widely used in many engineering applications for vibration mitigation and insulation and a very huge variety of anti-vibration systems are available, in which rubber-like materials are used for mechanical energy dissipation, such as in buffers, pads or mounts [1]. Special and unexpected properties may arise from the blending of polymer emulsions, depending on the miscibility and stability of the resulting blend. Therefore, the evaluation of their dynamic viscoelastic properties, in terms of complex elastic modulus and complex viscosity, is of paramount importance.

As known, the mechanical properties of a viscoelastic material cannot be univocally determined but depend on the adopted experimental method. Static, quasi-static and dynamic methods allow evaluating the mechanical properties in terms of a certain response related to a specific excitation: the ratio between the applied stress and the occurring deformation mainly depends on the nature of the applied stress itself and viceversa. As a consequence, specific methodologies should be designed and tailored as a function of the actual applications in which the material under investigation is used.

A wide number of methods in static, quasi-static and dynamic conditions are described in literature [2,3]. Static and quasi-static methods are valid for frequencies much smaller than the first resonance frequency of the considered system and are identified according to their loading type (compression/tension [4,5], torsion and pure shear [6]). Dynamic methods account for inertia effects and include longitudinal vibration excitation-based methods [7-11], bending vibration excitation-based method [12-15], shear vibration-based method [16,17] acoustical excitation-based methods [18-21], phase velocity measurement-based method [22].

Actually, none of these is suitable for the characterization on a wide frequency range of polymeric soft materials used for vibration isolation of systems that are approximated to a free-mass supported by a spring-damper system subjected to an underlying vibration, which is rather common in many industrial and medical applications. By way of example, in the field of precision engineering, many machines can only function properly as long as the vibration levels to which they are subjected do not exceed certain limits, or may even be damaged if subjected to excessive vibration [23]. Examples are optical benches using laser emissions, photoengraving benches for miniaturized circuits, as well as data centers with mechanical discs. Also, diagnostic imaging techniques such as computerized axial tomography, nuclear magnetic resonance, positron emission tomography, or investigation techniques such as electron microscopes and other techniques involving micrometric spatial resolutions, related to the medical field, fall into the category of machinery sensitive to vibrations. For this purpose, polymeric soft layers, mainly rubber- or polymer-based materials, are placed at the interface between the floor and the machines to suppress such vibration induced by the environment. The set of these elements can be approximated to a free loading-mass supported by a spring-damper system subject to an underlying vibration [24]. If these polymeric soft layers are tested in different conditions from the actual applications, consequent inaccuracies in the evaluation of their elastic and damping properties, such as the Young's modulus, the damping constant and the loss factor in dynamic conditions, might arise with the risk of compromising its correct use.

Furthermore, the evaluation of complex dynamic elastic modulus over an extended frequency allows implementing different models for the determination of other parameters (e.g. the Young's modulus at different temperatures according to the Williams, Landel and Ferry time-temperature superposition principle [6,25], the relaxation time in the Kelvin-Voigt model [26], etc).

In literature, besides resonant and non-resonant standard methods (e.g. ISO 9052-1:1989 [9], ISO 10846-3:2002 [27] and ISO 6721-10:2015 [17]), which are limited in frequency, two methods were presented for the evaluation of the viscoelastic properties on a wide frequency range of viscoelastic materials placed below a free-mass and subjected to an underlying vibration. The first is the work done by Kulik et al. (2009) [28,29] which uses a pseudo-spectral approximation of the wave equations to determine the complex Young's modulus of viscoelastic materials. The second is the work of Bonfiglio and Pompoli (2015) [30] which uses a transfer matrix approach to determine the values of the storage and loss moduli of viscoelastic materials in a wide frequency range.

In this paper, an improved supported free loading-mass method, based on the exact solution of the differential equation of the motion and suitable for the accurate characterization of the dynamic mechanical properties of polymeric soft materials placed between a free-mass and a vibrating plate over a wide frequency range with a high resolution, is investigated and applied to six different polymeric soft materials at INRiM (Italian National Institute of Metrological Research) vibration laboratory. Evaluation of the elastic and viscoelastic response, in terms of complex dynamic elastic modulus and complex dynamic viscosity, is achieved on small cylinder-shaped samples with a diameter of 30 mm over a wide frequency range from 25 Hz up to 1000 Hz and a resolution of 1 Hz. The frequency range in the present work is limited only by the characteristics of the available vibration exciter and accelerometer. Furthermore, this method might also be exploitable to characterize new generations of peculiar kinds of soft and ultra-soft polymer materials mainly used in biomedical engineering (such as hydrogel, biocompatible tissue-mimicking polymers, silicon-based and latex-based materials), where traditional techniques [9,27] are not always suitable for the accurate evaluations of their dynamic mechanical properties.

2. Material and methods

2.1 Materials

Six different samples of soft rubber-like materials designed for machinery anti-vibration purposes by *Arcobaleno2 S.p.A*, namely two samples of polychloroprene rubber, i.e. neoprene, (samples 1 and 2) and four samples of soft latex-silicone-based material (samples 3 to 6), are used to investigate the performance of the experimental technique here proposed. All samples are cylinders with a diameter d of 30 mm and different thicknesses L_0 and weights m, as shown in Figure 1 and Table 1. Width/thickness ratios range between 4 and 6.

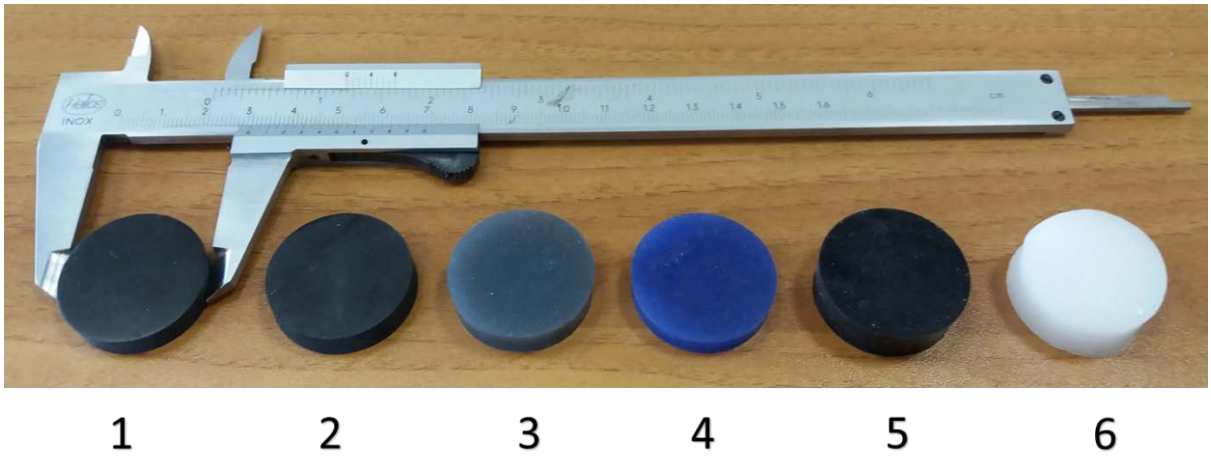


Fig. 1. The six samples of the polymeric soft materials tested in this work.

Table 1. Materials data

Material	Thickness L_0 / mm	Weight m /g	Density ρ/ kg/m^3
Sample 1	5.90	5.25	1259
Sample 2	6.48	6.36	1389
Sample 3	7.70	6.01	1105
Sample 4	6.20	4.99	1139
Sample 5	9.78	7.60	1100
Sample 6	9.46	5.48	820

2.2 Characterization of the materials according to standard methods

Initially, the six samples are characterized with three available standard methods for the evaluation of the viscoelastic properties in different conditions: shore-A hardness test according to ISO 48-4:2018 [31] for the evaluation of the elastic modulus in compression; unconfined uniaxial compression test according to ISO 604:2002 [4] for the evaluation of the quasi-static elastic modulus; rheological test following ISO 6721-10:2015 [17] for the determination of the complex shear and the elastic modulus. The first two can be considered as quasi-static methods, the third as a dynamic method.

All measurements of this work are carried out in laboratory-controlled environmental conditions with a temperature of (20.0±0.5) °C and relative humidity between 30 % and 50 %. Expanded uncertainties (at a confidence level of 95 %) are evaluated according to GUM [32], taking into account, as main uncertainty contributions, measurement repeatability and instrumental uncertainties.

2.2.1 Shore-A hardness

Shore-A hardness tests are performed according to ISO 48-4:2018 [31] with a standard Shore-A calibrated tester (*Affri*®) to measure the hardness of the rubber samples, as shown in Fig. 2. Shore-A hardness is measured

on the surface of the samples and its values can be converted into the elastic modulus E_H in compression, using the Kunz and Studer's formula [33], for polymeric elastomers:

$$E_H = \frac{1-\nu^2}{2r_d} \cdot \frac{0.549+0.07516 \cdot Sh_A}{0.025(100-Sh_A)} \cdot (2.6 - 0.02Sh_A) \quad (1)$$

where Sh_A is the Shore-A hardness, r_d is the tip radius of the durometer (0.395±0.005 mm) and ν is the Poisson's ratio is 0.475±0.025 for soft polymers [33-35]. This value can be conventionally considered as representative of soft rubber-like materials and is the main source of uncertainty, compared to the uncertainties due to the Shore-A hardness and to the tip radius of the durometer. In fact, an uncertainty of around 5 % on Poisson's ratio involves an uncertainty of around 5 % on the elastic modulus.

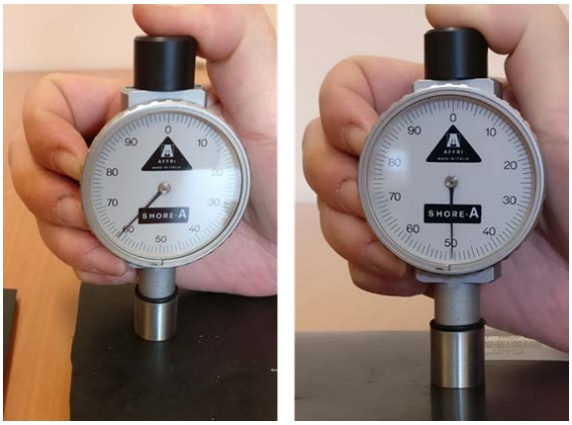


Figure 2: Shore-A calibrated tester.

Experimental results are reported in Table 2. On the basis of Eq. (1), the elastic modulus E_H in compression of the rubbers is also calculated, in MPa. It is found that sample 6 is much softer than the other samples.

Table 2. Shore-A experimental data with derived elastic modulus E_H.

Material	Shore A	E_H / MPa
Sample 1	52±1	5.68±0.26
Sample 2	70±1	9.11±0.45
Sample 3	29±1	3.04±0.16
Sample 4	33±1	3.44±0.17
Sample 5	41±1	4.29±0.20
Sample 6	5±1	0.95±0.10

2.2.2 Quasi-static unconfined uniaxial compression test

Quasi-static unconfined uniaxial compression tests are performed according to ISO 604:2002 [4], as shown in Fig. 3. In this setup, samples are compressed and the force response is measured by a load cell (resolution 1 mN) and the occurring deformation is measured by a linear encoder (resolution 0.1 μm). More information about the measurement system can be found in [36]. Since the materials are viscoelastic and the strain-rate may affect the force response, samples are compressed up to 10% of their height at a constant strain-rate of around $1.3 \cdot 10^{-2}$ s^{-1}, in order to evaluate quasi-static modulus at very low deformation rates. Stress-strain tests allow to evaluate the elastic modulus $E_{q\text{-}s}$, in quasi-static condition, by the best fit of experimental data in the linear region, on the basis of the following relation:

$$E_{\mathrm{q-s}} = \frac{F}{A} \cdot \frac{L_0}{dl} \tag{2}$$

where F is the measured force (N), A is the surface area (m^2) on which F is applied, L_0 is the initial thickness of the sample (m), dl is the occurring deformation length (m).



Fig. 3. The experimental setup for the quasi-static unconfined uniaxial compression tests.

By way of example, the full stress-strain experimental curves (black curve), with highlighted linear elastic regions (blue curve), of sample 1 and 6 are shown in the graphs of Fig. 4. Red lines are the best-fits of the elastic region. It can be easily shown the high work hardening of sample 6 compared to the other samples. In this case, the elastic modulus is highly strain-range dependent as shown in [37]. However, the most linear region of the curve was chosen for its evaluation. The quasi-static elastic modulus $E_{q\text{-}s}$ calculated with Eq. (2) of the tested materials are reported in Table 3.

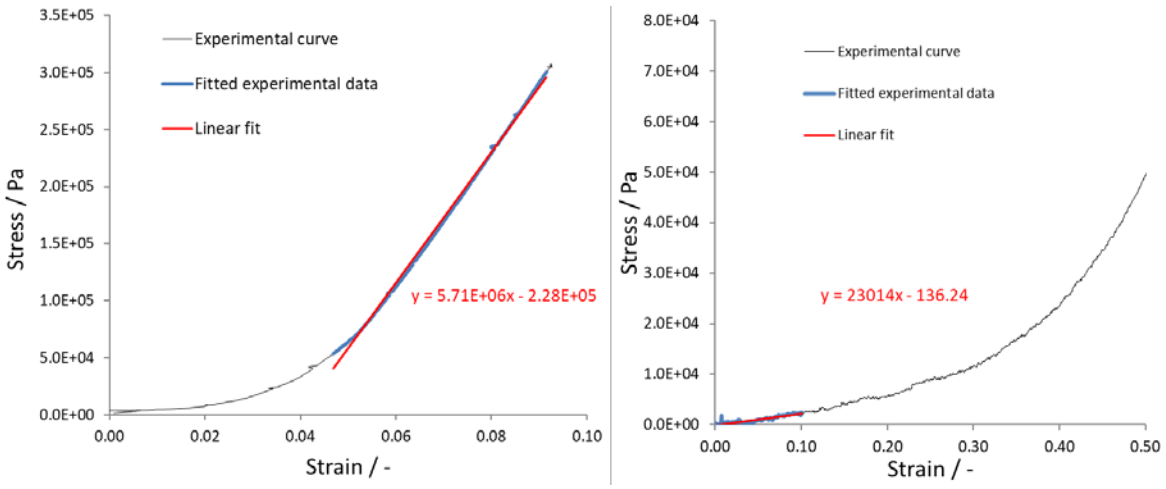


Fig. 4. Experimental results of quasi-static elastic modulus on sample 1 (left) and sample 6 (right).

Table 3. Experimental quasi-static elastic modulus $E_{q\text{-}s}$

Material	$E_{q\text{-}s}$ / MPa
Sample 1	5.71±0.23
Sample 2	10.93±0.11
Sample 3	1.96±0.11
Sample 4	2.32±0.04
Sample 5	2.84±0.10
Sample 6	0.02±0.01

2.2.3 Complex shear viscosity using a parallel-plate oscillatory rheometer

ISO 6721-10:2015 standard method is used to determine values of the dynamic rheological properties of polymer melts (complex shear viscosity η^*, dynamic shear viscosity η', the out-of-phase component of the complex shear viscosity η'', complex shear modulus G^*, shear loss modulus G'' and shear storage modulus G') by means of a rheometer.

In general terms, the elastic modulus E is the modulus of the complex elastic modulus E^* which is determined from the measurement of the complex shear modulus G^* as given by the following relation:

$$E^* = 2G^*(1 + \nu) \tag{3}$$

where ν is the Poisson's ratio, that, for the materials under study, is equal to 0.5.

The complex shear modulus G^* can be expressed as the sum of the storage modulus G' (real component) representing the elastic behavior of the material, i.e. stored deformation energy, and the loss modulus G'' (imaginary component) representing the viscous behavior, i.e. lost deformation energy, as follows:

$$G^* = G' + i \cdot G'', \quad (4)$$

but can be also defined as the ratio between the shear stress τ and the shear strain (deformation) γ,

$$G^* = \frac{\tau(t)}{\gamma(t)} \quad (5)$$

where $\tau(t) = \tau_0 \cos(\omega t + \delta)$ and $\gamma(t) = \gamma_0 \cos(\omega t)$. Indeed, the rheometer determines the quantities τ_0, γ_0 and δ, which can be expressed respectively as: the ratio between the shear force, F, and the area of the specimen experiencing the strain, A; the ratio between the transversal displacement of the upper plate, x, and the gap between the two plates, d; the shift between the stress applied on the material and its deformation [38].

In this work, the samples under investigation are characterized by means of a Thermoscientific Rheostress 6000 rheometer (shown in Fig. 5), using the oscillatory test method. The geometry used is the serrated plate-plate (P35 Ti L) with a diameter of 35 mm (PP35). The gap between the plates is dependent on the desired normal force, which is what is actually set.



Fig. 5. Thermoscientific Rheostress 6000 rheometer used for shear modulus measurements.

All measurements are carried out by setting the frequency and the shear stress and measuring the shear strain. The temperature is stabilized by connecting the rheometer to a liquid bath thermostat. Samples were tested applying a normal force of 0.75 N, similar to the force applied with the proposed method (Section 2.3), by setting the gap between the plates. Measurements, maintaining the shear stress at 20 Pa, are carried out at three different frequency values (0.1 Hz, 1 Hz, and 10 Hz), which are a compromise between the linear viscoelastic range of the material and the sensitivity of the instrument.

For each investigated sample, in Table 4 the determined rheometric dynamic elastic modulus E_{rheo} with the corresponding expanded uncertainty (k=2) is reported at the different frequencies. The uncertainty is determined by considering the repeatability of the measurement and the instrumental uncertainty.

Table 4. Experimental dynamic elastic modulus, E_{rheo}, obtained by rheometry at different frequencies, f.

Material	f / Hz	E_{rheo} / MPa
Sample 1	0.1	0.449±0.099
	1	0.500±0.113
	10	0.585±0.139
Sample 2	0.1	1.668±0.312
	1	1.944±0.443
	10	2.559±0.376
Sample 3	0.1	0.279±0.009
	1	0.289±0.020
	10	0.299±0.020
Sample 4	0.1	0.177±0.019
	1	0.178±0.032
	10	0.185±0.041
Sample 5	0.1	0.308±0.075
	1	0.309±0.068
	10	0.318±0.077
Sample 6	0.1	0.0090±0.0001
	1	0.0096±0.0001
	10	0.0110±0.0001

2.3 The proposed supported free loading-mass with vibrating base method

2.3.1 The physical model

The proposed measuring method is based on the determination of the motion of a single degree-of-freedom (SDOF) supported free loading-mass system with a sinusoidally excited vibrating base, as shown in Fig. 6.

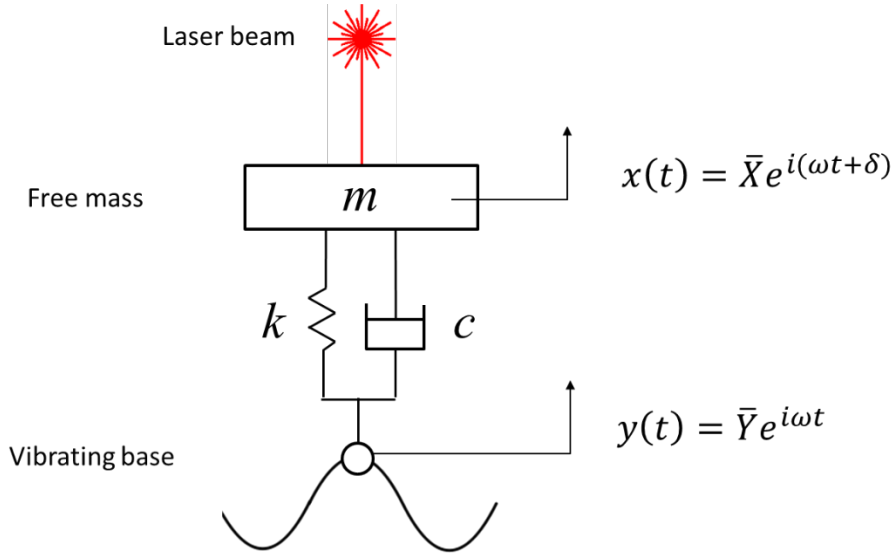


Fig. 6. Supported free loading-mass with a sinusoidally excited vibrating base.

The resulting motion of the free mass upon the polymeric soft material, i.e. $x(t)= \bar{X}e^{i(\omega t+\delta)}$, once forced by means of a sinusoidal oscillation of the base, i.e. $y(t)=\bar{Y}e^{i\omega t}$, depends on the elastic and damping properties of the polymeric soft material and it is described in terms of Newton's second law, from the following differential equation:

$$m\ddot{x} + c(\dot{x} - \dot{y}) + k(x - y) = 0 \tag{6}$$

where m is the free mass, in kg, c is the damping coefficient, in kg·s^{-1}, and k is the stiffness, in N·m.

By solving equation (6), in which the displacements of the loading-mass and the vibrating table are expressed in harmonic form, $x(t)= \bar{X}e^{i(\omega t+\delta)}$ and $y(t)=\bar{Y}e^{i\omega t}$, respectively, as shown in Fig. 6, it is possible to determine both the stiffness k and the damping coefficient c, as a function of the generated angular frequency ω, the base displacement amplitude $\bar{Y}$, the mass displacement amplitude $\bar{X}$ and the phase shift δ (all experimentally determined), as follows:

$$k = \frac{m\omega^2\bar{X}(\bar{X} - \bar{Y}\cos\delta)}{\bar{X}^2 + \bar{Y}^2 - 2\bar{X}\bar{Y}\cos\delta} \tag{7}$$

$$c = \frac{(m\omega^2 - k)\bar{X}\sin\delta}{\omega(\bar{X}\cos\delta - \bar{Y})} \tag{8}$$

Eqs. (7) and (8) allow evaluating, as a function of angular frequency ω of excitation, both the stiffness k and the damping coefficient c. The dynamic elastic modulus E_d is calculated from the stiffness k as a function of frequency, the area A (equal to $\pi d^2/4$ in this case of cylindrical samples) and the thickness L_0 of the polymeric

soft materials according to Eq. (9) [1]. In this way, it is possible to get the complex dynamic elastic modulus E_d^* as a function of the storage modulus E_d' and loss modulus E_d'' which are determined from the experimental phase shift δ according to Eqs. (10)-(12) [1].

$$E_d = |E_d^*| = k\frac{L_0}{A} \tag{9}$$

$$E_d' = E_d \cos\delta \tag{10}$$

$$E_d'' = E_d \sin\delta \tag{11}$$

$$E_d^* = E_d' + iE_d'' \tag{12}$$

From these parameters, it is possible to calculate the related dissipative properties of the polymeric soft materials under investigation, such as the complex dynamic viscosity η_d^* as function of η_d' and η_d'' which are determined from the loss modulus E_d'' and the storage modulus E_d', as shown in Eqs. (13)-(16):

$$\eta_d' = E_d''/\omega \tag{13}$$

$$\eta_d'' = E_d'/\omega \tag{14}$$

$$\eta_d^* = \eta_d' + i\eta_d'' \tag{15}$$

$$|\eta_d^*| = \sqrt{\eta_d'^2 + \eta_d''^2} = E_d/\omega \tag{16}$$

Combining the complex dynamic viscosity and the complex dynamic elastic modulus, the relaxation time τ as a function of frequency can be also obtained according to Eq. (17).

$$\tau = \frac{\eta_d''}{E_d''} = \frac{1}{\omega\ \tan\delta} \tag{17}$$

2.3.2 The measuring system

In Figs. 7 and 8 the measurement setup and the related SDOF supported free loading-mass system with a sinusoidally excited vibrating base are shown. A continuous sine sweep from 25 Hz to 1000 Hz is generated by a shaker (PCB electrodynamic shaker, model 2075E) for 4000 s (i.e. a frequency rate of 0.25 Hz/s) at a nearly-constant dynamic peak acceleration amplitude of 1 $m \cdot s^{-2}$ in order to guarantee an adequate signal to noise ratio at all frequencies of interest and to assure no detachment of the polymeric soft material or the free loading-mass from the contact surfaces during the oscillations. This is also checked by controlling the trend of the phase shift curve. In fact, if the mass detached from the specimen, its motion would be chaotic, even with transverse and rotational components, and the phase would be indeterminate. The polymeric soft material sample is placed between the vibrating base and the free mass at the center of the system. The free loading-mass is a stainless steel cylinder with a diameter identical to the diameter of the sample under test, i.e. 30 mm, a thickness of 10.00 mm and a weight of 56.13 g, i.e. an area density of 79.44 $kg \cdot m^{-2}$ and a static preload of

about 800 Pa. These parameters are chosen in order to be suitable for the available instrumentation, but can be arbitrarily changed depending on the application and the type of instrumentation used, therefore wider frequency ranges and higher resolutions could be achieved.

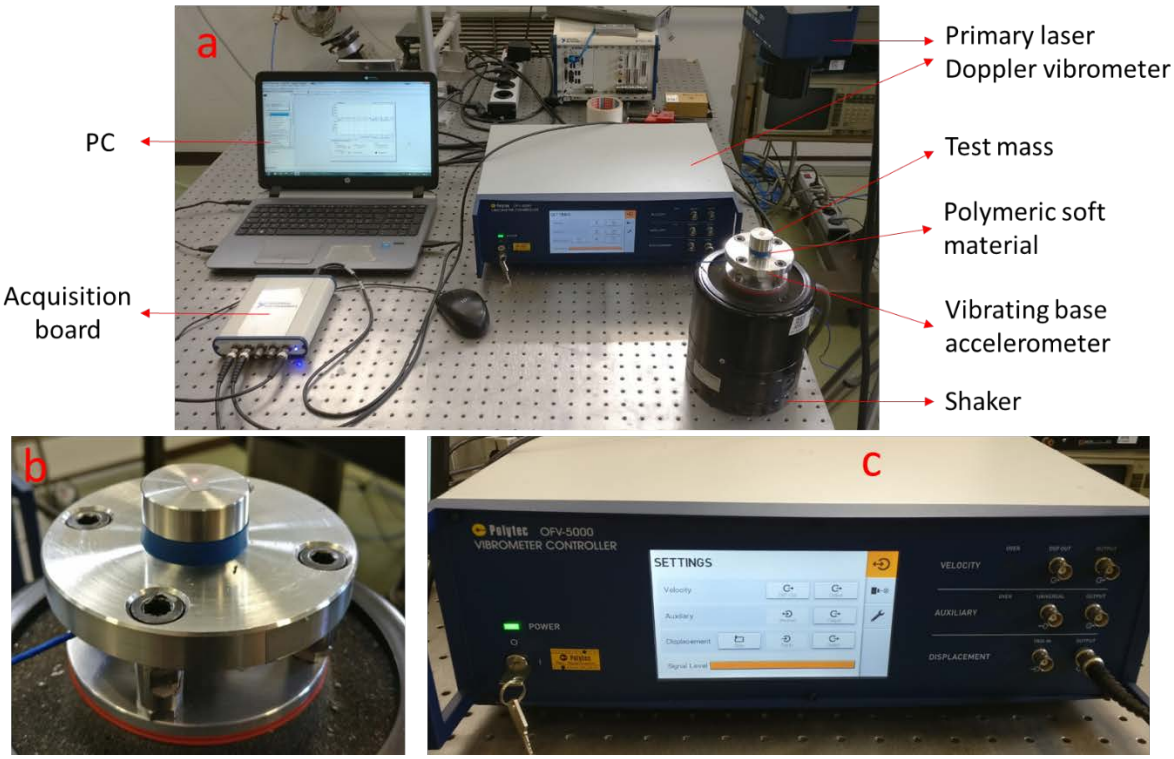


Fig. 7. The measurement setup: the instrumentation (a), the test mass and the polymeric soft material on the vibrating base (b), the vibrometer controller(c).

The dynamic displacement amplitude of the free mass $\bar{X}$ is directly measured by means of a primary laser Doppler vibrometer (Polytec OFV-505 sensor head and Polytec OFV5000 modular vibrometer, with an accuracy of $1 \cdot 10^{-9}$ m and a resolution of $0.2 \cdot 10^{-9}$ m) hitting the center of the upper surface of the test mass. The dynamic displacement amplitude of the vibrating base $\bar{Y}$ is obtained by performing the second derivative of the dynamic acceleration spectral signal (i.e. by dividing the dynamic acceleration spectrum by ω^2) measured by a fixed accelerometer (PCB model 080A199/482A23) placed below the vibrating base at its center. Both transducers have been previously calibrated against INRiM primary standards [39]. The two signals are acquired by an acquisition board NI 4431 with a sampling rate of 8192 Hz. Spectra and phase difference δ of the two signals as a function of frequency are computed in real-time through LabVIEW® Sound and Vibration tool software every second, thus with a frequency resolution of 1 Hz according to the ratio between the sampling rate (8192 Hz) and the number of FFT points (8192). All acquisition and spectral parameters can be directly set in the software. Since we generate a sweep signal with a frequency rate of 0.25 Hz/s, each spectrum, performed every second, corresponds to a frequency span of 0.25 Hz. Then, the average spectrum corresponding to a frequency span of 1 Hz is calculated as the average of four consecutive spectra. In order to get the complete spectrum of each signal from 25 to 1000 Hz, this operation is performed 1000 times in 4000 s.

An example of the real-time spectrum of the output voltage signals of the laser (free mass) and the accelerometer (vibrating base) computed in real-time through LabVIEW® Sound and Vibration tool software, measured with sample 4, is shown in Fig. 9. Voltage values are converted into meters (for the laser, i.e. free mass) or meters per squared second (for the accelerometer, i.e. vibrating base) using the calibration factor of the relevant instrument. These spectra are converted into displacement, according to the above-mentioned procedure, and are shown in the next Section (see Fig. 10). Measurements are performed for each sample five times in order to evaluate the contribution due to repeatability in the uncertainty assessment.

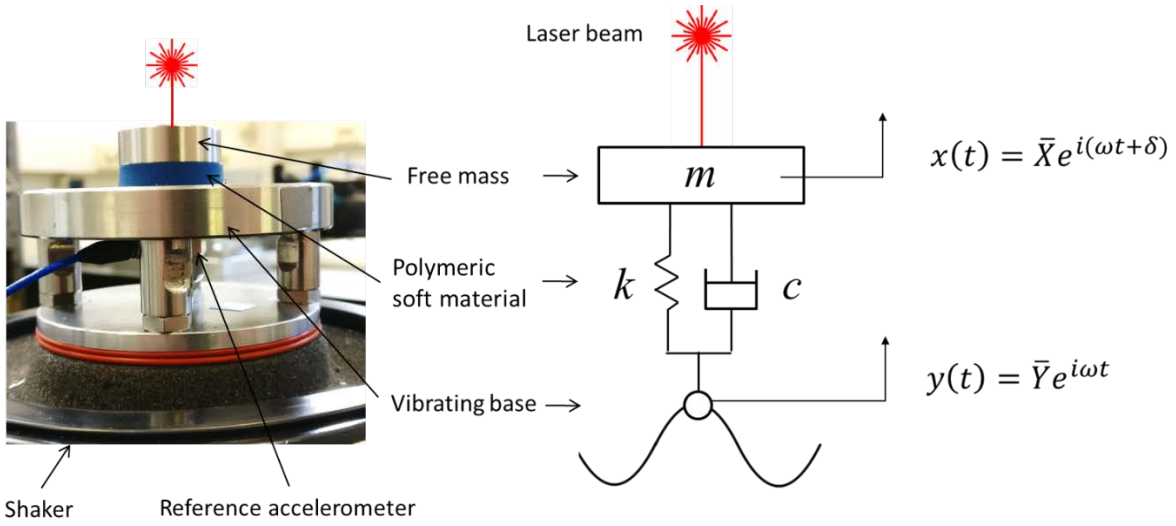


Fig. 8. The measurement system and SDOF mass-spring-damper model.

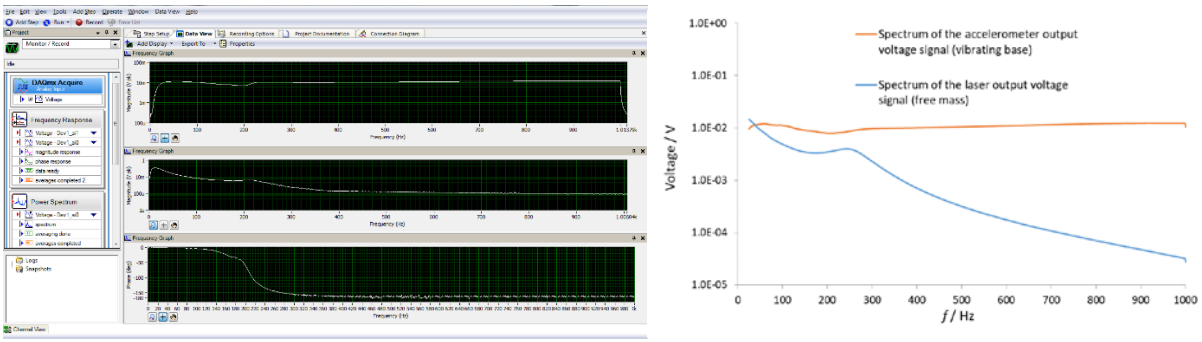


Fig. 9. Instrumental measurement display of the accelerometer (vibrating base) and laser (free mass) output voltage signals spectra and phase shift computed in real time by LabVIEW® Sound and Vibration tool software (left) and the corresponding data export used for calculation and analysis (right).

Preliminary tests are performed by means of a laser vibrometer in order to characterize the motion of the vibrating base in several positions, not only along the vertical direction of the motion but also along with transverse horizontal directions. As a matter of fact, transversal horizontal motions must be negligible with respect to the vertical one in order to be considered as an actual SDOF oscillating system. It is found that the

ratio between horizontal and vertical motions is, as average, around 1.2% in the whole frequency range, thus negligible for the scope of our work.

3. Results and discussion

3.1 Experimental results with the proposed method

Experimental results of measurements performed with the proposed method on the six samples are shown as follows. By way of example, the base displacement amplitude $\bar{Y}$, the loading-mass displacement amplitude $\bar{X}$ and the phase shift δ of the two signals as a function of frequency, evaluated for sample 4 (first repetition), is shown in Fig. 10. Displacements decrease as a function of frequency since a nearly-constant acceleration of around 1 m/s^2 is set for the whole extended frequency range. This value assures that the contact between the shaker, the mass, and the soft material is not broken. Moreover, the displacements of the mass and of the vibrating base start diverging from the resonant frequency of the spring-damper-mass system (258 Hz for sample 4) when the phase shift is 90°, as expected.

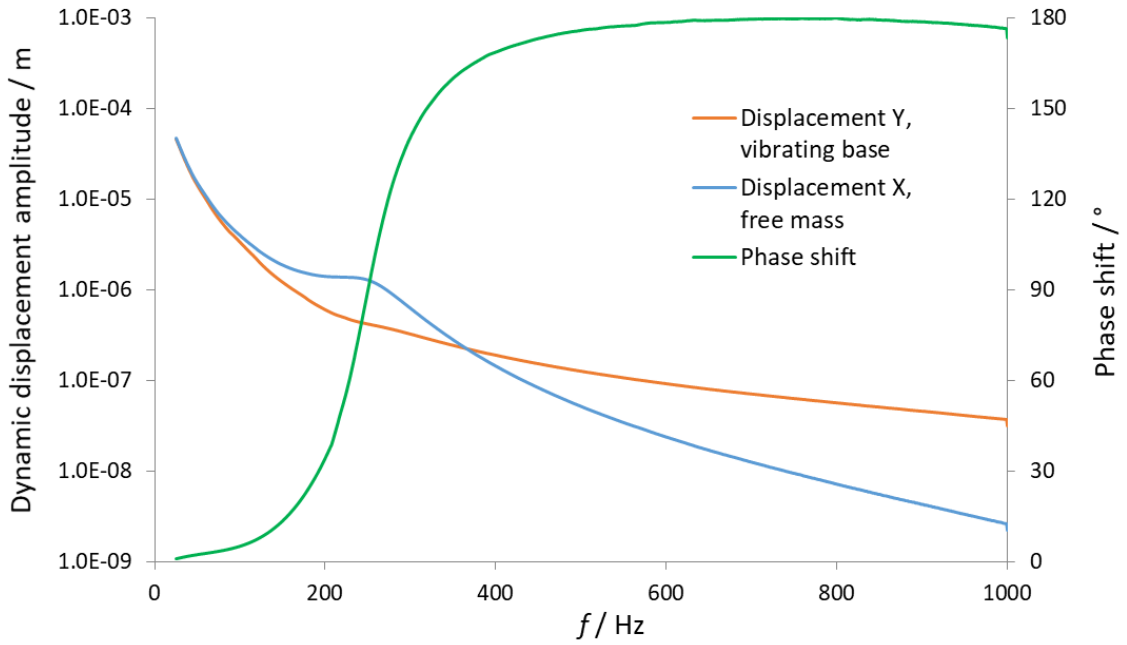
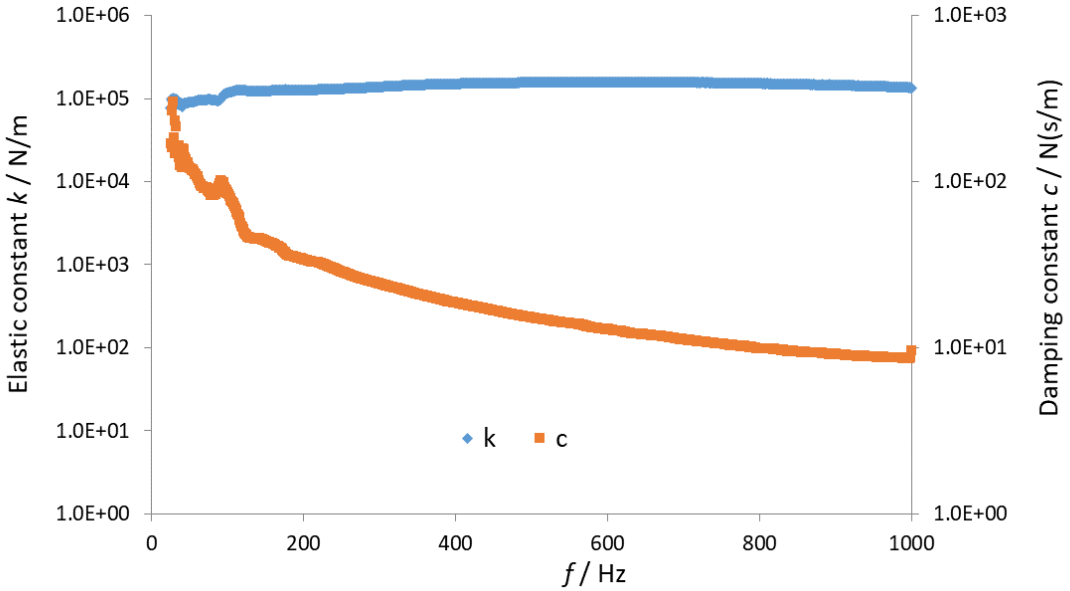


Fig. 10: Base displacement amplitude, loading-mass displacement amplitude and phase shift δ, as a function of frequency, of sample 4.

From these measurements, it is possible to get the stiffness k and the damping coefficient c, according to Eqs. (7) and (8). By way of example, k and c curves of sample 4 as a function of frequency (first measurement repetition) are shown in Fig. 11.

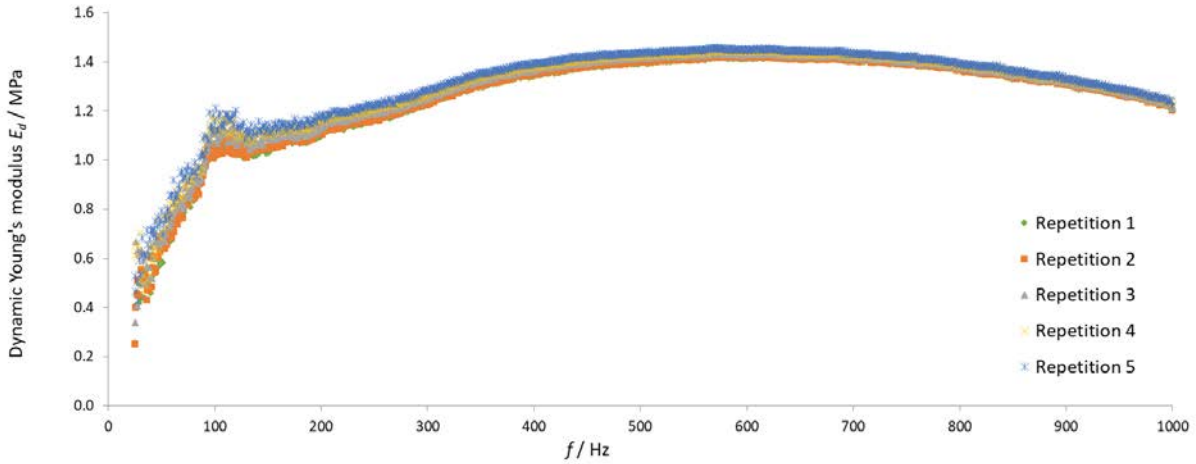


322

323 *Fig. 11. Stiffness k and damping coefficient c as a function of frequency of sample 4.*

324

325 By applying Eqs. (9)-(17), the dynamic elastic modulus E_d, the storage modulus E_d', loss modulus E_d'', the
326 modulus of the complex dynamic viscosity $|\eta_d^*|$ and the relaxation time τ as a function of frequency are obtained
327 for each sample and for each measurement repetition. By way of example, five repeated measurements of
328 dynamic elastic modulus E_d on sample 4 are reported in Fig. 12. No systematic increase or decrease between
329 the repetitions or drift over time is found, thus the variability is mainly due to random errors.



330

331 *Fig. 12. The dynamic elastic modulus E_d as a function of frequency of sample 4 from five repeated*
332 *measurements.*

333

334 Mean values and standard deviations are then computed from the five measurement repetitions in order to
335 get, for each parameter, a single curve with its associated uncertainty (see Section 3.2 for details). In Figs. 13-
336 17, mean experimental curves of the dynamic elastic modulus E_d, the storage modulus E_d', the loss modulus

E_d'', the modulus of the complex dynamic viscosity $|\eta_d^*|$ and the relaxation time τ as a function of frequency for the six tested materials are shown. It is worth noting that the dynamic elastic modulus E_d and the modulus of the complex dynamic viscosity $|\eta_d^*|$ are phase shift independent, while the storage modulus E_d', the loss modulus E_d'' and the relaxation time τ are phase shift dependent, as shown in the relevant equations. This means that, at the resonances (i.e. when the phase shift is equal to 90°), a particular behaviour of the curves related to the phase shift-dependent quantities is expected. At these frequencies, the deformations of the material are over-forced by the resonant amplification and the material does not store elastic energy and all the mechanical work is converted into heat, therefore the highest value of loss modulus and the lowest value of storage modulus and relaxation time are expected. This behaviour depends on the experimental setup and, in particular, on the used free loading-mass. A change in the loading-mass value would result in a shift along the frequency axis of the peaks or dips of the relevant quantities.

Values of the dynamic elastic modulus E_d for all tested samples slowly and linearly increase with frequency, as expected (see Fig. (13)), since the elastic response of rubbers is directly proportional to rate, as known. Sample 6 shows lower values of E_d compared to the others as already observed in preliminary standard measurements. At low frequencies, the slight dispersion of data is higher due to the high sensitivity of the vibrating system to small phase shift values and to similar displacements of the mass and the vibrating base below the resonant frequency of the spring-damper-mass system. Storage modulus E_d' (Fig. 14) and the loss modulus E_d'' (Fig. 15) show similar behavior. The first shows dips occurring around the resonant frequency of the spring-damper-mass system, as expected. The modulus of the complex dynamic viscosity $|\eta_d^*|$ (Fig. (16)) reflects the trend of the curve of E_d divided by the angular frequency ω. The relaxation time τ curves (Fig. (17)) show an exponential decrease as a function of frequency with dips occurring at the resonant frequencies of the different samples, as expected. Resonant frequencies for the different samples are listed in Table 5.

Table 5. Experimental resonant frequencies of the spring-damper-mass system with the different materials.

Material	f_{res} / Hz
Sample 1	191
Sample 2	420
Sample 3	197
Sample 4	258
Sample 5	237
Sample 6	43

An attempt to eliminate the influence of the resonances in the storage modulus E_d', loss modulus E_d'' and relaxation time τ curves is carried out by performing a second-order polynomial fit for the first two curves and a decreasing exponential fit, before the resonant frequency, and a logarithmic fit, after the resonant frequency, fits for the last one. An example is shown for sample 4 in Figs. 18, 19 and 20, related to the storage modulus E_d', loss modulus E_d'' and relaxation time τ, respectively.

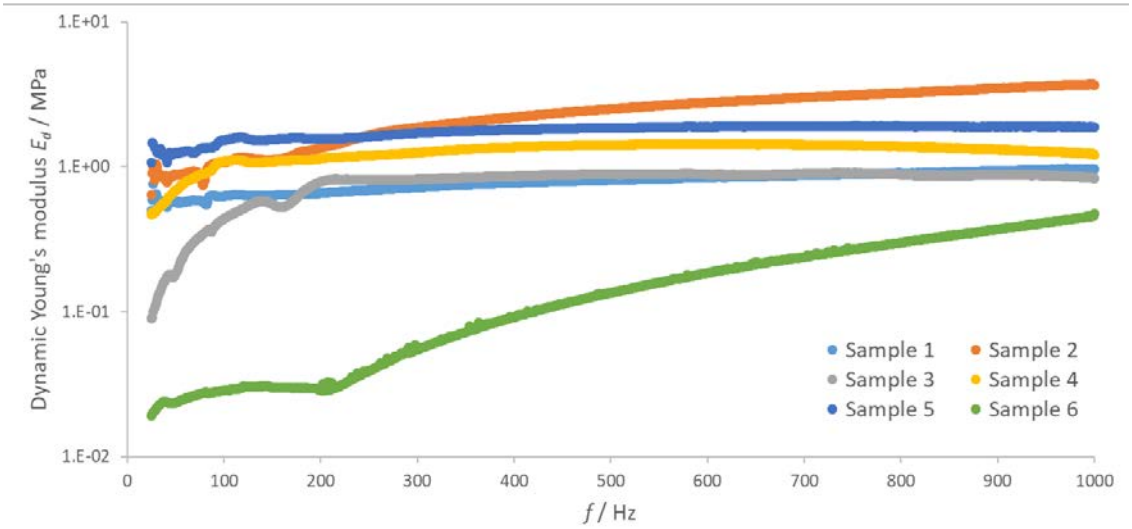


Fig. 13. The dynamic elastic modulus E_d as a function of frequency of the six samples.

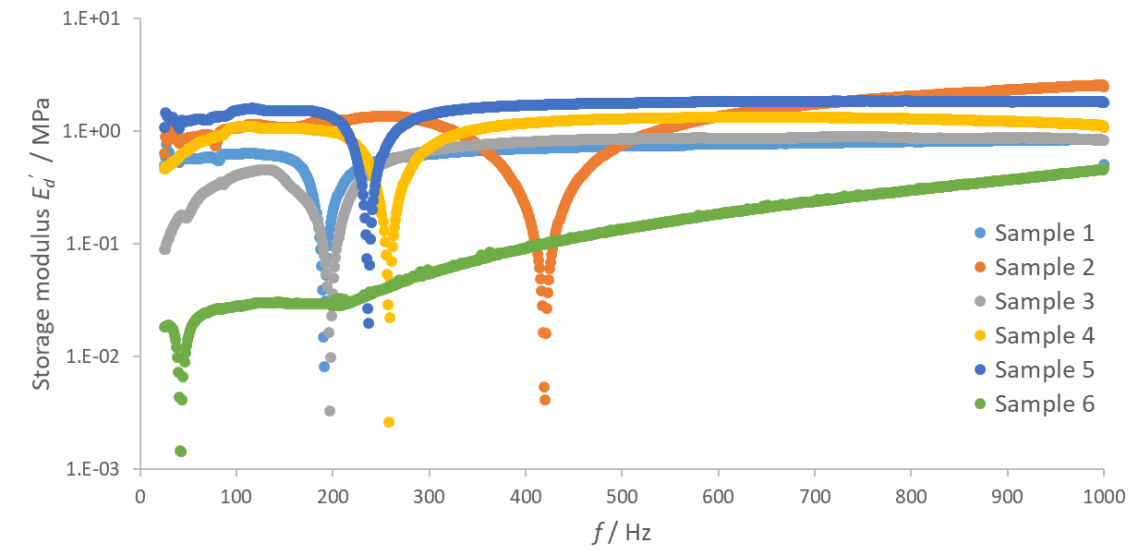


Fig. 14. The storage modulus E_d' as a function of frequency of the six samples.

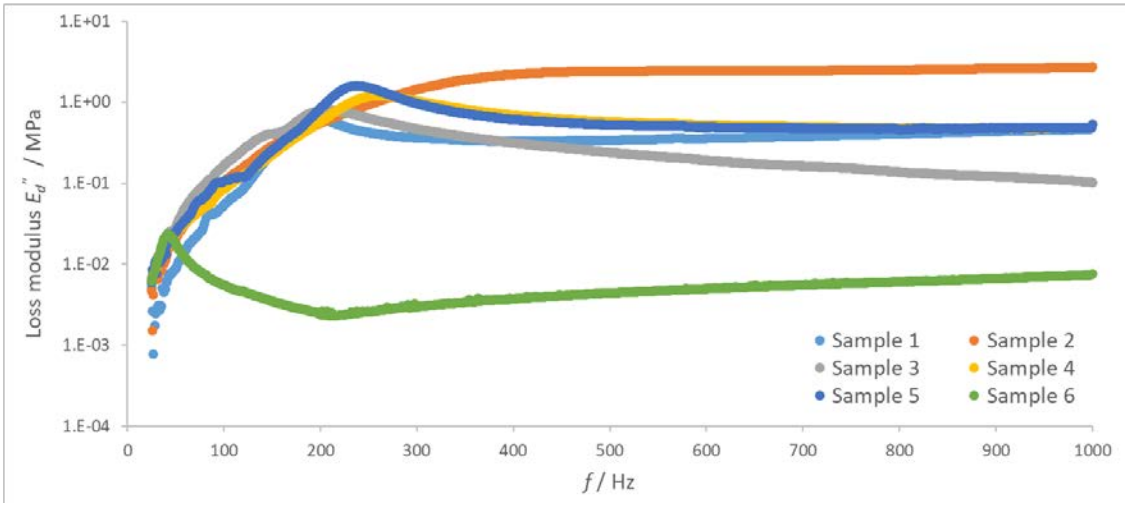
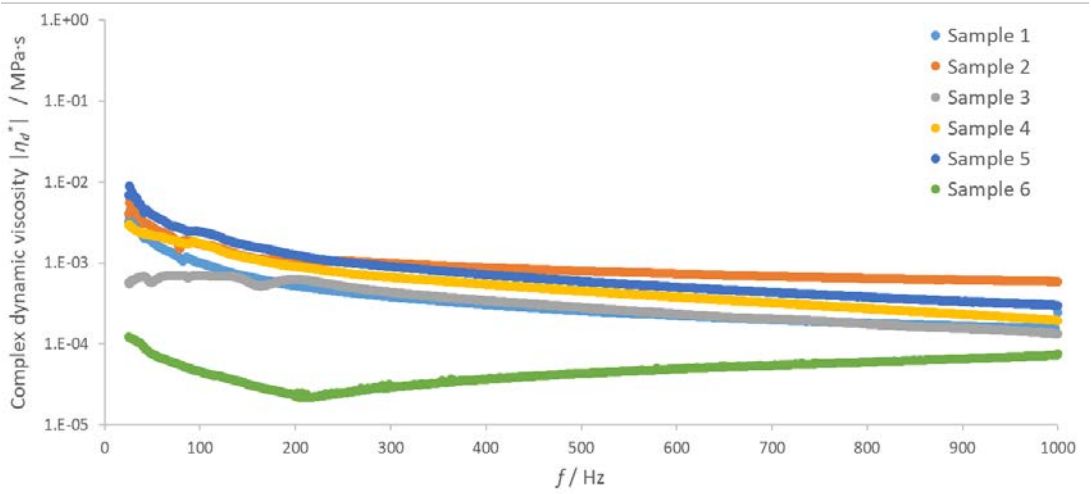


Fig. 15. The loss modulus E_d'' as a function of frequency of the six samples.

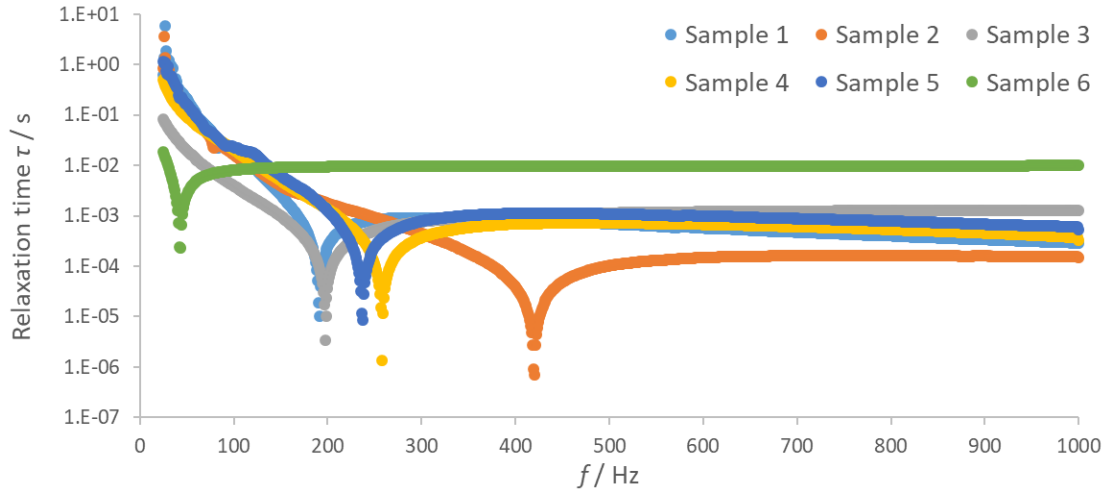


376

377 *Fig. 16. The modulus of the complex dynamic viscosity $|\eta_d^*|$ as a function of frequency*

378 *of the six samples.*

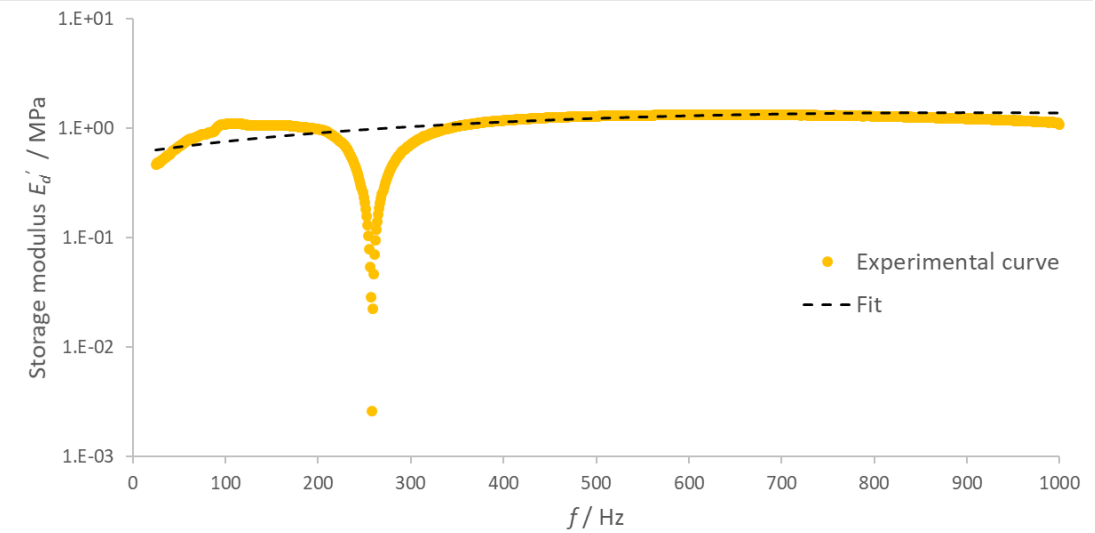
379



380

381 *Fig. 17. The relaxation time τ as a function of frequency of the six samples.*

382



383

384 *Fig. 18. Fit of the storage modulus E_d' curve as a function of frequency for sample 4.*

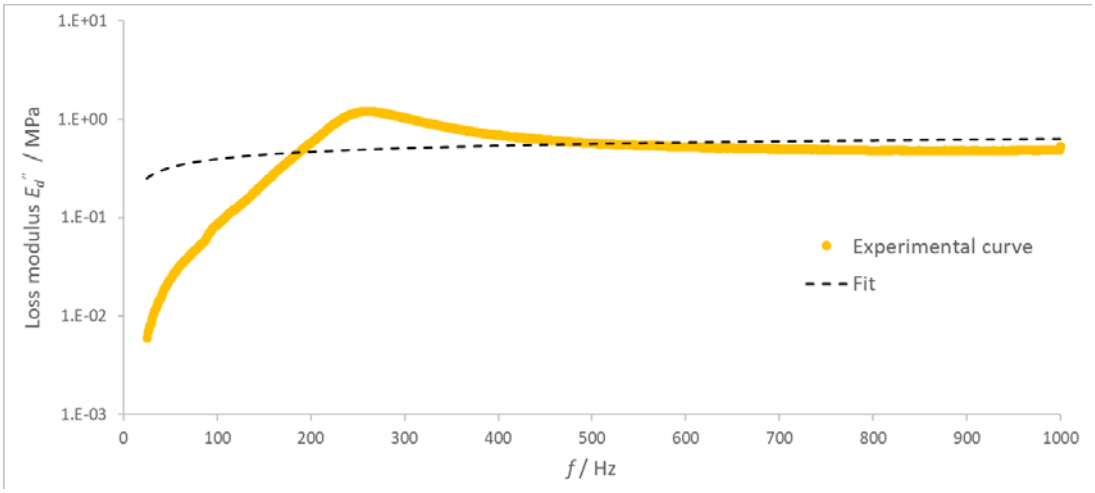


Fig. 19. Fit of the loss modulus E_d'' curve as a function of frequency for sample 4.

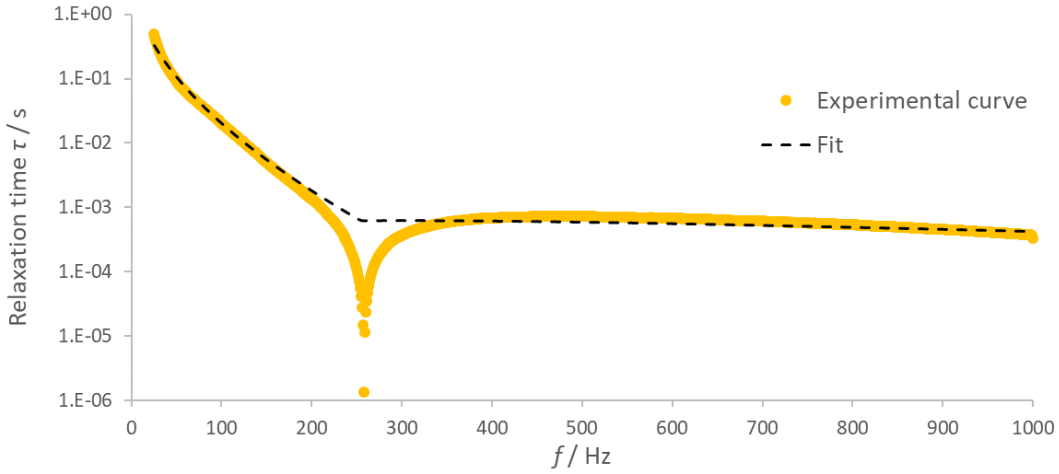


Fig. 20. Fit of the relaxation time τ curve as a function of frequency for sample 4.

3.2 Uncertainty assessment of the proposed method

Uncertainty assessment is performed according to GUM [32] by considering the instrumental uncertainty contribution u_{instr} and the standard deviation obtained from five repeated measurements s_{rep}. By way of example, the uncertainties associated with the dynamic elastic modulus E_d as a function of frequency for sample 4 are considered. Similar uncertainty results are found for all tested materials. Standard uncertainty due to the instrumentation exponentially decreases as a function of frequency from 1.7 % at 25 Hz up to 0.05 % at 1000 Hz in terms of relative uncertainties as shown in Fig. 21. On average, it is around 0.2 %. An example of instrumental uncertainty assessment at 500 Hz is shown in Table 6, where the sources of uncertainty taken into account are the tolerance intervals or the calibration uncertainties. The quantity $u^2(x_j)$ represents the variance of the uncertainty contributions of the independent variables x_j, c_j is the sensitivity coefficient, $u_j^2(E_d)$ is the combined variance of the elastic modulus E_d obtained for each uncertainty contribution, and $u_{instr}(E_d)$ is the instrumental combined standard uncertainty associated to E_d, evaluated by applying the law of uncertainty propagation according to GUM [32]. In this specific case, a relative standard uncertainty of 0.1 % is found.

Table 6. Instrumental uncertainty associated with the dynamic elastic modulus E_d of sample 4 at 500 Hz.

Independent variables x_j		**$u^2(x_j)$**	**Note**	**c_j**	**$u_j^2(E_d)$**
Symbol / Unit	**Value**				
L_0 / m	$6.41 \cdot 10^{-3}$	$8.3 \cdot 10^{-12}$	Tolerance	$2.2 \cdot 10^{2}$	$4.1 \cdot 10^{-7}$
d / m	$3.00 \cdot 10^{-2}$	$8.3 \cdot 10^{-12}$	Tolerance	$-9.4 \cdot 10^{1}$	$7.4 \cdot 10^{-8}$
m / kg	$5.61 \cdot 10^{-2}$	$8.3 \cdot 10^{-12}$	Tolerance	$2.5 \cdot 10^{1}$	$5.3 \cdot 10^{-9}$
f / Hz	$5.00 \cdot 10^{2}$	$3.3 \cdot 10^{-3}$	Tolerance	$5.7 \cdot 10^{-3}$	$1.1 \cdot 10^{-7}$
$\bar{X}$ / m	$1.60 \cdot 10^{-4}$	$6.4 \cdot 10^{-15}$	Calibration	$6.6 \cdot 10^{3}$	$2.8 \cdot 10^{-7}$
$\bar{Y}$ / m	$3.92 \cdot 10^{-4}$	$3.8 \cdot 10^{-14}$	Calibration	$-2.7 \cdot 10^{3}$	$2.8 \cdot 10^{-7}$
δ / °	$1.56 \cdot 10^{2}$	$8.3 \cdot 10^{-14}$	Tolerance	$3.3 \cdot 10^{-3}$	$9.0 \cdot 10^{-7}$
E_d / MPa	1.42			**$u_{instr}(E_d)$ / MPa**	$1.4 \cdot 10^{-3}$

Standard deviation due to repeatability $s_{rep}(E_d)$ exponentially decreases from around 10 % at 25 Hz to around 0.5 % at 1000 Hz, as shown in Fig. 21. On average, it is around 1.4 %. In general terms, instrumentation uncertainty is much lower than repeatability for increasing frequency. This means that the major uncertainty contribution is due to the intrinsic variability of the measurand itself rather than instrumentation. By performing the square root of the sum of the squares of the two terms, $u_{instr}(E_d)$ and $s_{rep}(E_d)$, multiplied by a coverage factor k of 2 (at a confidence level of 95 %), the overall expanded uncertainties $U(E_d)$ are calculated as a function of frequency as shown in Fig. 19. Values decrease from around 20 % at 25 Hz to around 1 % at 100 Hz. On average, expanded uncertainty is around 2.8 %.

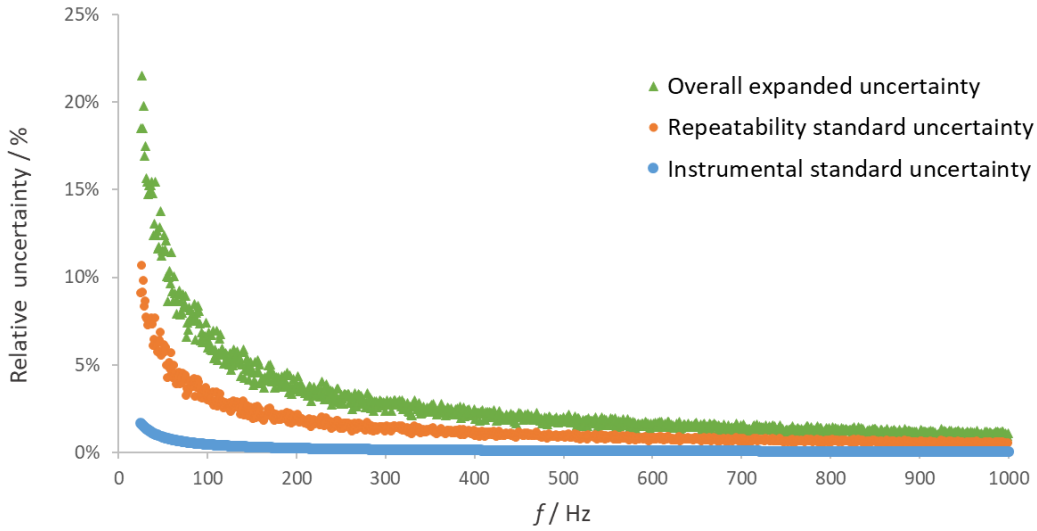


Fig. 21. Repeatability uncertainty (orange), instrumental uncertainty (blue) and overall expanded (k=2) uncertainty (green) associated with the dynamic elastic modulus of sample 4 as a function of frequency.

3.3 Comparison between different measurement methods

It is known that the elastic and damping properties of viscoelastic materials depend on the applied experimental methods. Nonetheless, a first qualitative attempt to compare elastic modulus results of the proposed method with the standard ones, previously described in Section 2.2, is performed. It is worth noting that the proposed method and the rheological method allow evaluating the dynamic modulus whereas the Shore-A and compression test methods assess a quasi-static modulus. Comparisons for all tested materials are reported in Figs. 22-27. In general terms, it is found that quasi-static modulus, evaluated with Shore-A method and compression tests, is higher than the dynamic modulus, evaluated with the rheological and the proposed method, as found in literature on viscoelastic polymers with low elastic moduli [40-42]. This, besides the different mechanical excitation of the samples from the two methods, can be due to the fact that small strains are generated with the dynamic methods (around 0.01 %) compared to the quasi-static one (around 10 %). This causes a different response of the viscoelastic materials that are strain-range dependent, showing a stiffer modulus at increasing strain [37,43]. Such behavior is related to the time-temperature dependent properties of polymers as described by the work of Williams, Landel, and Ferry [25], and deepened in Section 3.4.

In addition, quasi-static elastic moduli evaluated with the Shore-A method and compression tests are consistent, as expected [44]. Also comparison between dynamic elastic modulus curves evaluated with the rheological method and the proposed one, although the different frequency ranges and the different mechanical excitations, show consistent results within the declared uncertainty level. Such evidence allows a first metrological validation of the method. It is also found that elastic modulus measured in the extended frequency range increases at increasing frequencies. This has been explained by the fact that a dynamic stress applied at a high frequency can be seen as a stress applied at a high strain rate, and at an increasing strain rate, the molecular mobility of the polymer chains decreases by making the chains stiffer [45].

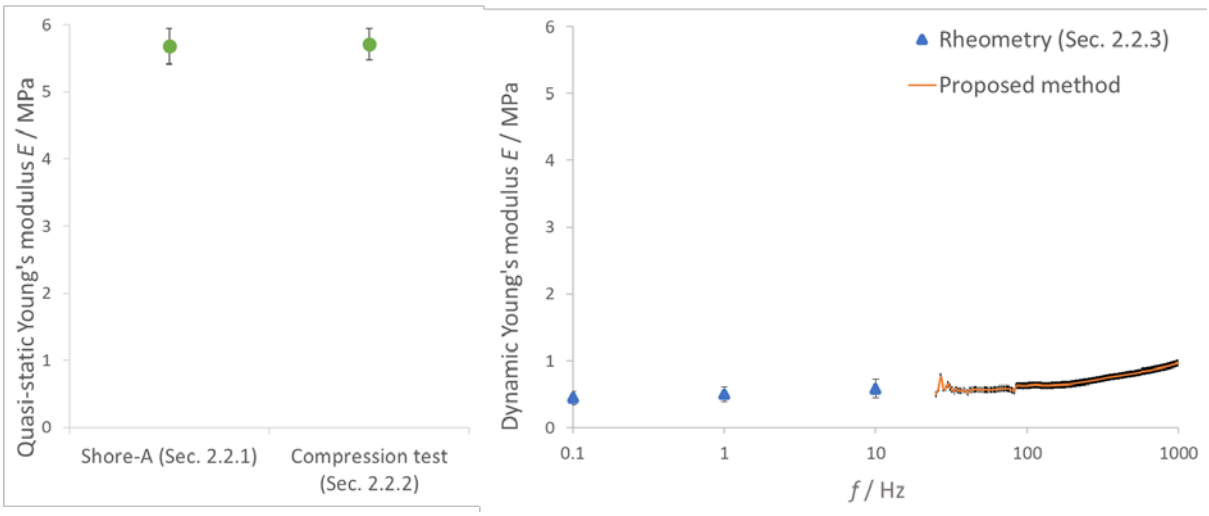
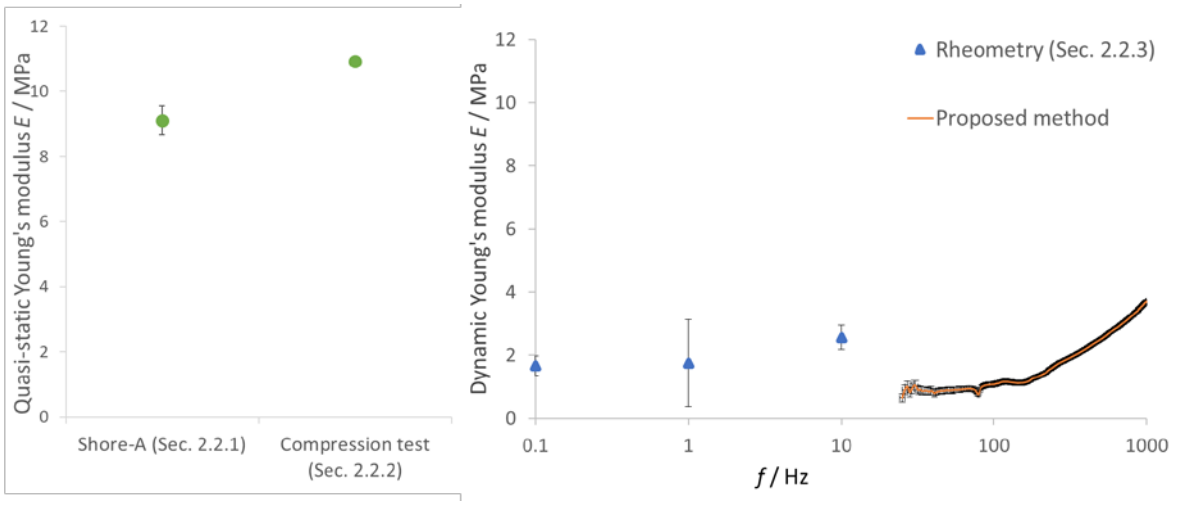


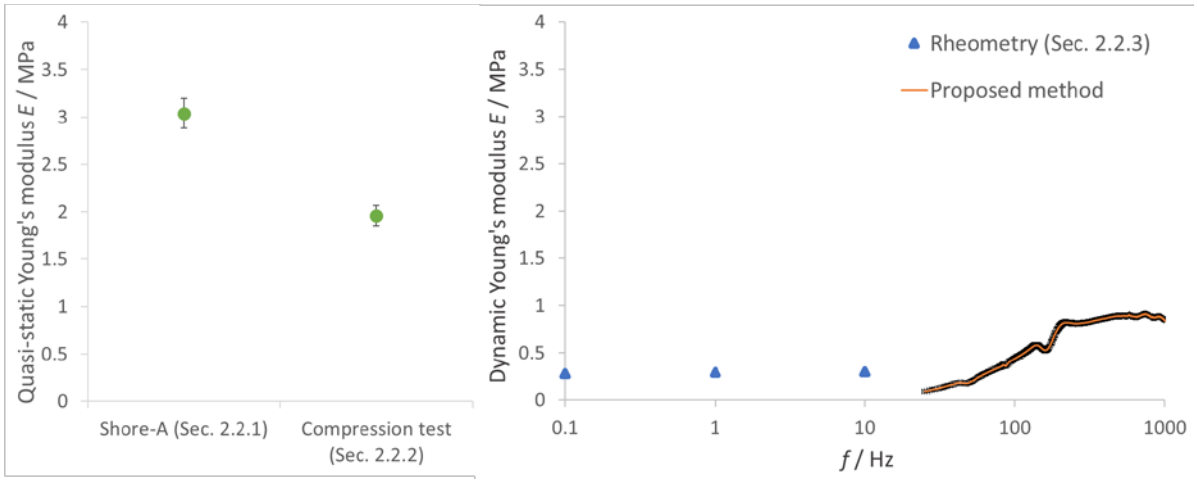
Fig. 22. Comparison between different measurement methods for sample 1.



447

448 *Fig. 23. Comparison between different measurement methods for sample 2.*

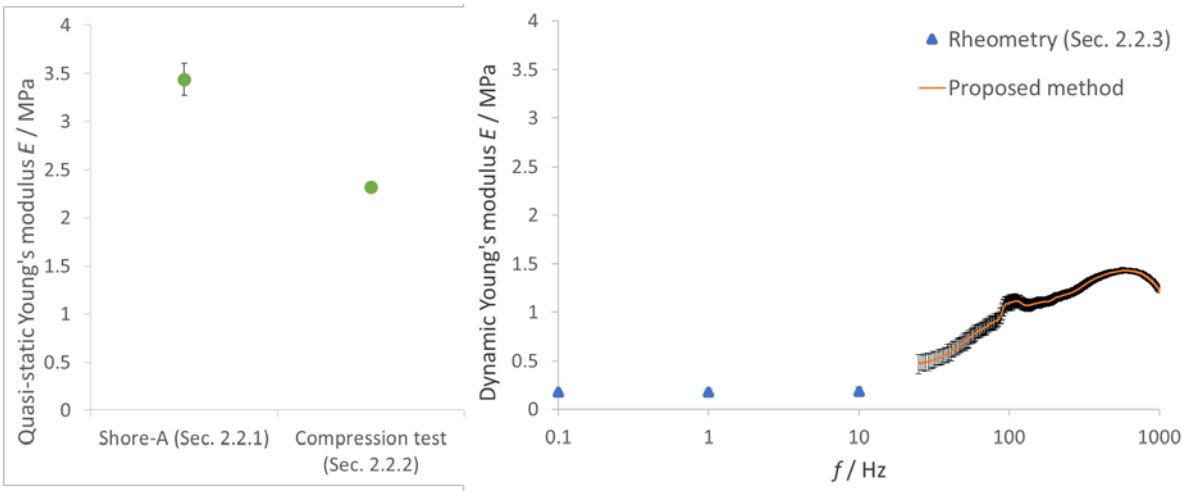
449



450

451 *Fig. 24. Comparison between different measurement methods for sample 3.*

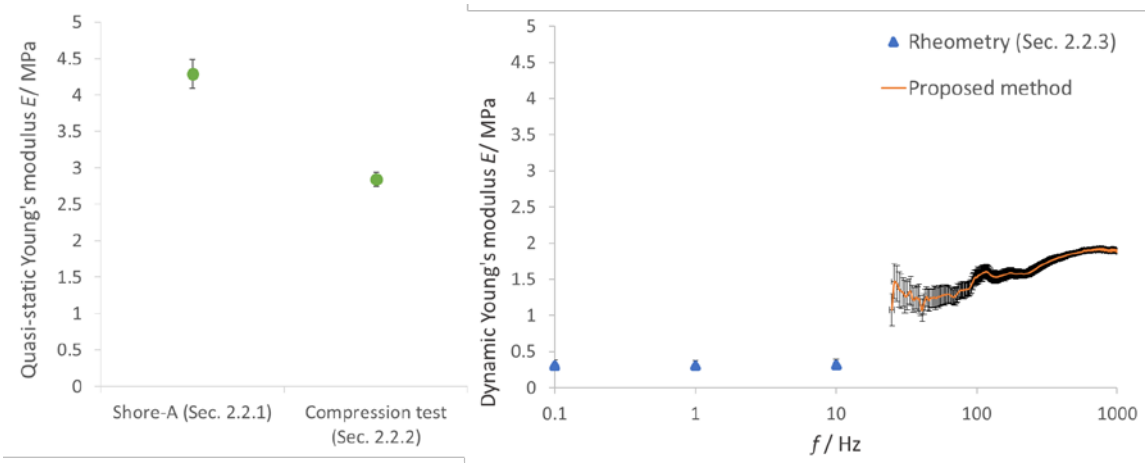
452



453

454 *Fig. 25. Comparison between different measurement methods for sample 4.*

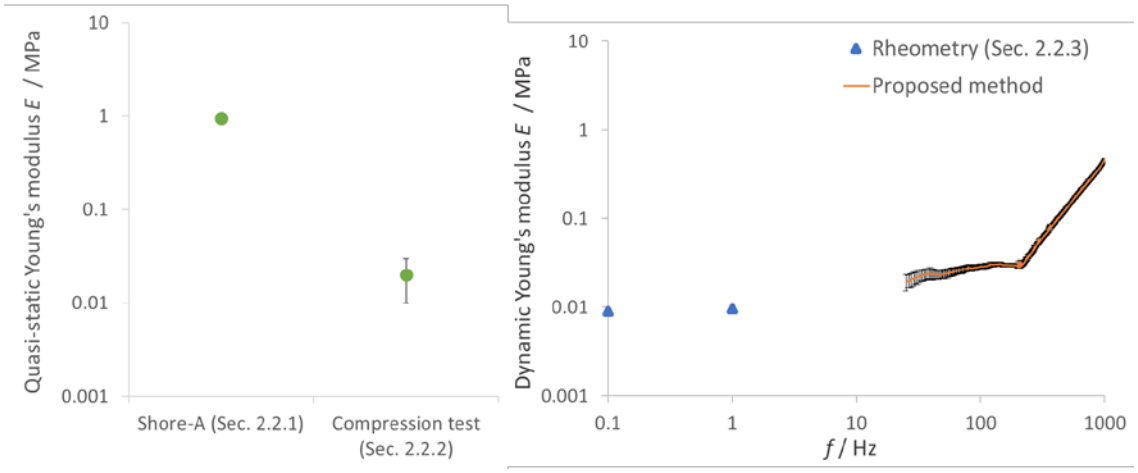
455



456

457 *Fig. 26. Comparison between different measurement methods for sample 5.*

458



459

460 *Fig. 27. Comparison between different measurement methods for sample 6.*

461

462 **3.4 Time-temperature superposition principle**

463 As stated in the introduction, an extended frequency range allows to shift data measured on a narrower
464 frequency range at various temperatures according to the time-temperature superposition (TTS) principle [25].
465 The method consists in translating horizontally and vertically the curves of E as a function of frequency,
466 obtained on a reduced frequency range at different temperatures in order to superimpose them at a given
467 temperature T_0 (see Fig. 28 as an example [6]).

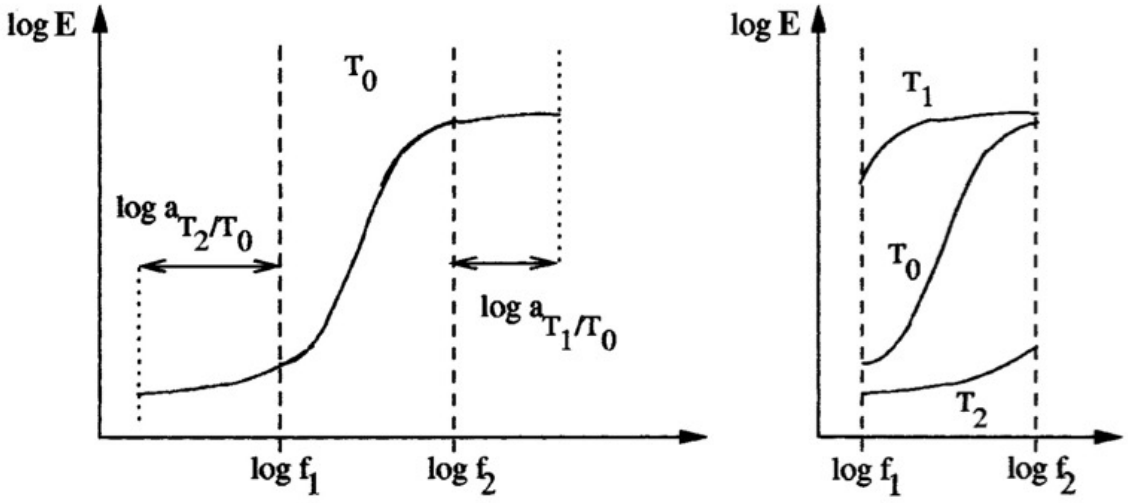


Fig. 28. Time-temperature superposition principle [6].

Reducing frequency is equivalent to increasing temperature and vice versa. This method can be generalized according to Eq. (18) [6].

$$E(T_i, \omega) = b_{T_i/T_0} E(T_0, a_{T_i/T_0}\omega) \tag{18}$$

where $a_{Ti/T0}$ is equal to the ratio of relaxation times at temperatures T_i and T_0 and $b_{Ti/T0}$ is the ratio of the material density at temperatures T_i and T_0 and often is equal to 1 due to the low density variations [6]. The term $a_{Ti/T0}$ has to be experimentally determined as a function of temperature and represents the horizontal shift factor allowing isotherms to overlap with adjacent isotherms, thereby constructing the master curve of the response. This equation is valid only for temperatures higher than the glass transition temperature T_g.

By way of example, the time-temperature superimposition principle is applied to sample 1 starting from the experimental values as a function of frequency from 25 Hz to 1000 Hz. Since no relaxation time measurements are performed at different temperatures, values of $a_{Ti/T0}$ from Trovedi and Siviour (2020) [46] measured on a type of neoprene very similar to sample 1 are used. Starting from a reference temperature of 20 °C, as our case, which is higher than its glass transition temperature T_g (around -36 °C), they found that $\log(a_{Ti/T0}) = 2.17\text{-}0.108 \cdot T$, where T is the temperature in °C.

Considering a reference temperature of 20 °C and the 100-200 Hz frequency range, the elastic modulus isothermal curves are built for $a_{Ti/T0}$ values of ¼, ½, 2 and 4, which corresponds to temperatures of around 26 °C, 23 °C, 17 °C and 15 °C and frequency ranges of 25-50 Hz, 50-100 Hz, 200-400 Hz and 400-800 Hz, respectively. The curves are constructed by shifting to the left the part of the master curve corresponding to higher frequencies (i.e. a lower temperature than the reference one) and by shifting to the right the part of the curve corresponding to lower frequencies (i.e. a higher temperature than the reference one). The isothermal curves of sample 1 are constructed from the dynamic elastic modulus master curve (Fig. 13) and are shown in

Fig. 29 for a reference temperature of 20 °C and a frequency range of 100-200 Hz. It is found the typical behavior of the dynamic elastic modulus which decreases as a function of temperature and increases as a function of frequency [2,45-48]. This example confirms the usefulness of the proposed method over a wide frequency range to obtain the master curves at different temperatures with high resolution.

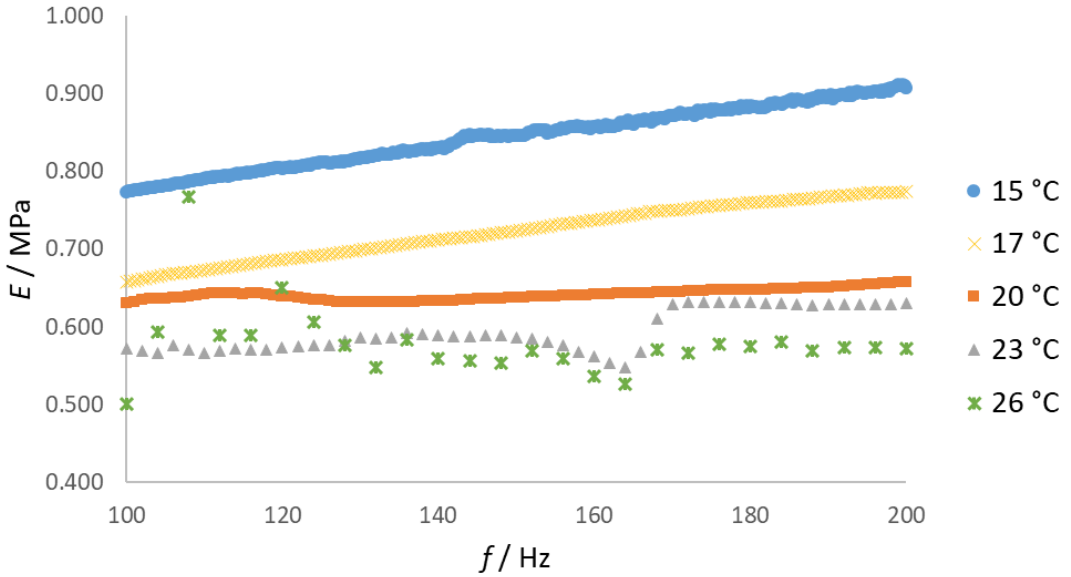


Fig. 29. Isotherms showing the frequency and temperature dependence of dynamic elastic modulus between 100 Hz and 200 Hz for sample 1.

4. Conclusions

In this work, an experimental method to determine the complex dynamic elastic modulus of soft materials used for vibration isolation of systems, which can be approximated to a free-mass supported by a spring-damper system subjected to an underlying vibration, is shown and described. The proposed method is applied to six polymeric soft materials over a frequency range between 25 Hz and 1000 Hz and a resolution of 1 Hz. These boundary conditions are chosen in order to be suitable for the available instrumentation but can be arbitrarily changed depending on the application and the type of instrumentation used, therefore wider frequency ranges and higher resolutions could be achieved. The six samples were previously characterized with two quasi-static standard methods (Shore-A, quasi-static stress-strain) and a dynamic one (rheometry). With the proposed method, the dynamic elastic modulus, the storage modulus, the loss modulus, the complex viscosity and the relaxation times as a function of frequency are evaluated for the six tested materials. Results show the typical viscoelastic increase of elastic modulus as a function of frequency. Uncertainty assessment is performed according to GUM by considering the instrumental uncertainty and the repeatability. It is found that the instrumental uncertainty is negligible with respect to repeatability depending on the measurand itself. Relative expanded uncertainties, on average of about 3 %, exponentially decrease as a function of frequency. Dynamic elastic modulus results are then compared to the results obtained by means of quasi-static and dynamic standard methods. In general terms, it is shown a good agreement within the uncertainty ranges

between values resulting from the dynamic methods and those determined using the new method described in this work, whereas systematic differences are found in comparison with quasi-static measurements, as expected for such viscoelastic materials. The method presented here, providing measurements over a wide frequency range and with a high resolution, can also be used to evaluate the master curves at higher or lower temperatures, compared to the experimental one, in a narrower frequency range using the time-temperature superposition principle, as shown, by way of example, for sample 1.

In the future, more polymeric soft materials will be tested with different loading-masses in order to evaluate their influence on the elastic and damping behavior, possibly with a new system to reach lower frequencies. In addition, new generations of peculiar kinds of soft and ultra-soft polymer materials mainly used in biomedical engineering (such as hydrogel, biocompatible tissue-mimicking polymers, silicon-based and latex-based materials) will be tested with this system to investigate their elastic properties since standard ones, in dynamic conditions, are not feasible for brittle and ultra-soft materials. In particular, any power dependence in the proposed methodology will be investigated.

References

[1] J.D. Ferry, Viscoelastic Properties of Polymers, third ed., Wiley, 1980.

[2] L. Jaouen, A. Renault, M. Deverge, Elastic and damping characterizations of acoustical porous materials: available experimental methods and applications to a melamine foam, Appl. Acoust., 69 (12) (2008), pp. 1129-1140.

[3] V. M. Kulik and A. V. Boiko, Physical principles of methods for measuring viscoelastic properties, Journal of Applied Mechanics and Technical Physics, 59 (5) (2018), pp. 874–885.

[4] ISO 604:2002, Plastics— Determination of compressive properties.

[5] M. Melon, M. Mariez, C. Ayrault and Sahraoui, Acoustical and mechanical characterization of anisotropic open-cell foam, J Acoust Soc Am, 104 (1998), pp. 2622-2627.

[6] M. Etchessahar, L. Benyahia, S. Sahraoui and J.-F. Tassin, Frequency dependence of elastic properties of acoustics foams, J Acoust Soc Am, 117 (2005), pp. 1114-1121.

[7] ISO 6721-4:2019, Plastics — Determination of dynamic mechanical properties — Part 4: Tensile vibration — Non-resonance method.

[8] ISO 6721-12:2009, Plastics — Determination of dynamic mechanical properties — Part 12: Compressive vibration — Non-resonance method.

[9] ISO 9052-1:1989, Acoustics — Determination of dynamic stiffness — Part 1: Materials used under floating floors in dwellings.

[10] T. Pritz, Dynamic Young's modulus and loss factor of plastic foams for impact sound isolation, J. Sound Vib., 178 (1994), pp. 315-322.

[11] L. E. Ooi, Z. M. Ripin, Dynamic stiffness and loss factor measurement of engine rubber mount by impact test, Materials & Design, 32(4) (2011), pp. 1880-1887.

[12] J.L. Wojtowicki, L. Jaouen and R. Panneton , A new approach for the measurement of damping properties of materials using the Oberst beam, Rev. Sci. Instrum., 75 (8) (2004), pp. 2569-2574.
[13] ASTM E756 - 05(2017), Standard Test Method for Measuring Vibration-Damping Properties of Materials.
[14] M. Etchessahar, Caractérisation mécanique en basses fréquences des matériaux acoustiques, PhD thesis, Université du Maine, Le Mans, France, 2002.
[15] R. Caracciolo, A. Gasparetto, M. Giovagnoni, An experimental technique for complete dynamic characterization of a viscoelastic material, J. Sound Vibrat., 272 (2004), pp. 1013-1032.
[16] ISO 6721-6:2019, Plastics — Determination of dynamic mechanical properties — Part 6: Shear vibration — Non-resonance method.
[17] ISO 6721-10:2015, Plastics — Determination of dynamic mechanical properties — Part 10: Complex shear viscosity using a parallel-plate oscillatory rheometer.
[18] V. Andreev, V. N. Dmitriev, Y. Pishchalnikov, O. Rudenko, O. Sapozhnikov, A. Sarvazyan, Observation of Shear Waves Excited by Focused Ultrasound in Rubber-Like Medium, Acoust. Phys., 43 (2) (1997), pp. 123–128.
[19] N. Sellen, Modification de l'impédance de surface d'un matériau par contrôle actif: application à la caractérisation et l'optimisation d'un absorbant acoustique, PhD thesis, Ecole Centrale de Lyon, France, (2003).
[20] J. S.Vaddi, S. D. Holland, M. R. Kessler, Loss modulus measurement of a viscoelastic polymer at acoustic and ultrasonic frequencies using vibrothermography, Measurement, 168(15) (2021), pp. 108311.
[21] Y. Y. Kim, Young's modulus measurement of a silicon nitride thin-film using an ultrasonically actuated microcantilever, Measurement 115 (2018) 133-138.
[22] L. Boeckx, P. Leclaire, P. Khurana, C. Glorieux, W. Lauriks and J.-F. Allard, Investigation of the phase velocities of guided acoustic waves in soft porous layers, J. Acoust. Soc. Am., 117 (2005), pp. 545-554.
[23] D. B. DeBra, Vibration Isolation of Precision Machine Tools and Instruments, CIRP Annals, 41(2) (1992), pp. 711-718.
[24] K. Mori, D. Kono, I.Yamaji, A. Matsubara, Vibration Reduction of Machine Tool Using Viscoelastic Damper Support, Procedia CIRP, 46 (2016), pp. 448-451.
[25] M. L. Williams, R. F. Landel, J. D. Ferry, The temperature dependence of relaxation mechanisms in amorphous polymers and other glass-forming liquids, J. Am. Chem. Soc., 77(14) (1955), pp. 3701–3707.
[26] W. Li-li, One-Dimensional Visco-Elastic Waves and Elastic-Visco-Plastic Waves, Foundations of Stress Waves, Elsevier 2007.
[27] ISO 10846-3:2002, Acoustics and vibration — Laboratory measurement of vibro-acoustic transfer properties of resilient elements — Part 3: Indirect method for determination of the dynamic stiffness of resilient supports for translatory motion.
[28] V.M. Kulik, B.N. Semenov, A.V. Boiko, B.M. Seoudi, H.H. Chun, I. Lee, Measurement of dynamic properties of viscoelastic materials, Exp. Mech., 49 (2009), pp. 417-425.

592 [29] A. V. Boiko, V. M. Kulik, B. M. Seoudi, H.H. Chun, I. Lee, Measurement method of complex viscoelastic
593 material properties, International Journal of Solids and Structures, 47 (2010), pp. 374–382.
594 [30] P. Bonfiglio, F. Pompoli, Determination of the dynamic complex modulus of viscoelastic materials using
595 a time domain approach, Polymer Testing, 48 (2015), pp. 89-96.
596 [31] ISO 48-4:2018, Rubber, vulcanized or thermoplastic — Determination of hardness — Part 4: Indentation
597 hardness by durometer method (Shore hardness).
598 [32] JCGM 100:2008, Evaluation of measurement data — Guide to the expression of uncertainty in
599 measurement
600 [33] J. Kunz, M. Studer, Determining the modulus of elasticity in compression via Shore-A hardness,
601 Kunststoffe international, 96(6) (2006), pp. 92-94.
602 [34] P. H. Mott, C. M. Roland, Limits to Poisson's ratio in isotropic materials, Physical review B, 80(13),
603 (2009), 132104.
604 [35] M. L. Anderson, P. H. Mott, C. M. Roland, The compression of bonded rubber disks. Rubber chemistry
605 and technology, 77(2), (2004), pp. 293-302.
606 [36] A. Schiavi, A. Prato, Evidences of non-linear short-term stress relaxation in polymers, Polymer Testing,
607 59 (2017), pp. 220-229.
608 [37] A. Schiavi, R. Cuccaro, A. Adriano, Functional mechanical attributes of natural and synthetic gel-based
609 scaffolds in tissue engineering: strain-stiffening effects on apparent elastic modulus and compressive
610 toughness, Journal of the Mechanical Behavior of Biomedical Materials, 126, 105066, 2022.
611 [38] T. G. Mezger, The Rheology Handbook, 3rd Revised Edition, Hanover: Vincetz Network (2011).
612 [39] M. Galetto, A. Schiavi, G. Genta, A. Prato, F. Mazzoleni, Uncertainty evaluation in calibration of low-
613 cost digital MEMS accelerometers for advanced manufacturing applications, CIRP Annals, 68(1) (2019), pp.
614 535-538.
615 [40] E. Tomasetti, R. Legras, B. Nysten, Quantitative approach towards the measurement of polypropylene/
616 (ethylene-propylene) copolymer blends surface elastic properties by AFM, Nanotechnology, 9(4) (1998), pp.
617 305.
618 [41] E. Mfoumou, C. Hedberg, S. Kao-Walter, Static versus low frequency dynamic elastic modulus
619 measurement of thin films, Electronic Journal «Technical Acoustics», 17 (2006).
620 [42] A. Schiavi, A. Prato, F. Mazzoleni, Dynamic stiffness of resilient materials based on accurate
621 measurement of dynamic force and dynamic displacement, The 25th International Congress on Sound and
622 Vibration, Hiroshima, Japan, 2018.
623 [43] G. E. Warnaka, H. T. Miller, Strain-Dependent Properties of Polymers, Rubber Chemistry and
624 Technology, 39(5) (1966), pp. 1421–1427.
625 [44] A. Schiavi, A. Prato, Elastic and viscoelastic properties of synthetic rubber (polychloroprene): dynamic
626 and static characterization, The 24th International Congress on Sound and Vibration, London, UK, 2017.
627 [45] J. Richeton, S. Ahzi, L. Daridon, Y. Rémond, A formulation of the cooperative model for the yield stress
628 of amorphous polymers for a wide range of strain rates and temperatures, Polymer, 46 (2005), pp. 6035-6043.

[46] A.R. Trivedi, C.R. Siviour, A novel methodology for predicting the high rate mechanical response of polymers from low rate data: application to (plasticised) poly(vinyl chloride), Mech. Time-Depend Mater (2020).
[47] N. Dusunceli, An observation of the evolution of equilibrium stress on poly(lactic acid) and poly(lactic acid)/hydroxyapatite nanocomposites, Proceedings of the Institution of Mechanical Engineers, Part C: Journal of Mechanical Engineering Science, 235(6) (2021), pp. 1026-1044.
[48] J. Li, J. Zhang, Shuo Chen, Study on dynamic viscoelastic properties and constitutive model of non-water reacted polyurethane grouting materials, Measurement, 176 (2021) 109115.